Interpretation of Frequency Response Analysis for Fault Detection in Power Transformers

Salem Mgammal Al-Ameri [1] , **Muhammad Saufi Kamarudin** [1,*] , **Mohd Fairouz Mohd Yousof** [1,*] , **Ali A. Salem** [1] , **A. Abu Siada** [2] **and Mohamed I. Mosaad** [3]

[1] Department of Power Electrical, Faculty of Electrical and Electronic Engineering, University Tun Hussein Onn Malaysia, Batu Pahat 86400, Johor, Malaysia; salemawadh@uthm.edu.my (S.M.A.-A.); eng.alisalem20@gmail.com (A.A.S.)

[2] Electrical and Computer Engineering Department, Curtin University, Bentley, WA 6152, Australia; a.abusiada@curtin.edu.au

[3] Electrical and Electronics Engineering Technology Department, Yanbu Industrial College (YIC), Alnahdah, Yanbu Al Sinaiyah, Yanbu 46452, Saudi Arabia; m_i_mosaad@hotmail.com

* Correspondence: saufi@uthm.edu.my (M.S.K.); fairouz@uthm.edu.my (M.F.M.Y.)

Abstract: Frequency response analysis (FRA) is a method of monitoring a power transformer's mechanical integrity. However, identifying the type of fault and its severity by comparing measured responses is still challenging and mostly relies on personnel expertise. This paper is taking one step forward to standardize the FRA interpretation process by proposing guidelines based on various international standards and FRA case studies. In this study, the FRA signature is divided into three regions: low-, mid- and high-frequency regions. The deviation from the fingerprint signature for various faults is classified into small, large, and no variations, based on the calculation of the correlation coefficient. The proposed guidelines are developed based on the frequency regions, and the level of variation is represented using a simple arrow method to simplify the interpretation process. A case study is conducted on a three-phase 11/0.433 kV, 500 kVA distribution transformer with a short circuit winding fault to validate the proposed guidelines.

Keywords: transformer faults; frequency response analysis; interpretation; correlation coefficient

1. Introduction

Frequency response analysis (FRA) is the most reliable diagnostic tool for detecting winding and core deformation in power transformers [1]. Such deformations affect the equivalent, inductive, and capacitive components of the transformer, thereby altering its frequency response. Currently, an expert is required to analyze the obtained results, which makes the interpretation process inconsistent and reliant more on personnel expertise than standardized guidelines. Essentially, FRA is a comparative technique that requires a reference signature (fingerprint) with which future signatures are compared, to identify any changes due to various internal faults. In case the reference signature is not available, a comparison with the response of other phases of the same transformer or with the response of an identical transformer (sister unit) is conducted. Although international standards such as the IEEE standard [1], the CIGRE standard [2], the IEC standard [3], and the DL/T 911 standard [4] are available, there are still difficulties in identifying and quantifying transformer winding faults [5]. The other drawback of the FRA technique as a diagnostic tool is that standard procedures do not yet define the measured data.

For identifying and quantifying various transformer faults, numerical indices are used, such as the correlation coefficient (CC). Sum square error (SSE) or mean squared error (MSE), the absolute sum of logarithmic error (ASLE), minimum-maximum ratio (MM), and spectrum deviation (SD) have also been presented in the literature [6–8]. The CC can calculate the variation between two FRA traces. If the two responses are identical,

the CC is 1; otherwise, it is 0. The CC is sensitive to changes in response resonance and anti-resonance frequencies, and it is widely used for FRA. The SSE can show the deviation between normal and faulty responses. The ASLE is highly recommended in the latest studies and is reported to be more pertinent than the SSE. SD has also been used to detect variation between frequency responses for normal power transformers and winding deformation [9]. Typically, SD shows similar sensitivity to the ASLE.

On the other hand, some methods have been proposed for a more objective interpretation of FRA measurements, as elaborated below.

Past studies adopted a transformer-equivalent high-frequency circuit by representing the winding using resistance, inductance, and capacitance (RLC) ladder circuit [10–12], due to the difficulty of staging physical faults on real transformers. The equivalent circuit enables understanding of the changes in response due to specific faults that might otherwise be impossible to reproduce on actual winding. Several transformer faults can be simulated using the equivalent circuit, including short circuit turns, inter-disk deformation, axial displacement, buckling faults, bushing and insulation faults, and clamping pressure loss [13–15].

In the mathematical models presented in the literature, the frequency response is modeled as a rational function with actual coefficients. For comparison purposes, the parameters of the model can be indicated, but their sensitivity to various types of faults is not stated [16,17]. The disadvantage of using this numerical method is the time-consuming nature of solving complex mathematical equations [18].

The use of artificial neural networks (ANNs) to identify transformer failure is also reported. Essentially, ANNs are used to estimate transformer parameters over a wide frequency range. ANNs are also used as a complementary technique to statistical indicators to improve the FRA interpretation process's reliability [19,20].

Digital image processing has been used on 2D and 3D FRA plots to extract unique features for each fault type [21]. In [21], a three-dimensional-FRA trace in one plot that includes frequency, magnitude, and phase is presented. Compared to the current interpretation practice, which relies only on the magnitude plot, more features can be extracted from the proposed 2D and 3D FRA signature, hence increasing the accuracy of the FRA classification.

Previous works in [22–24] investigate the impact of winding deformation, bushing, and inter-disk faults on the FRA signature. The effects of tap changer variation and the loss of clamping pressure on the FRA signature were also studied in [25–29]. These studies were based on statistical indicators and necessary visual inspection. A comparison between the latest proposed methods for FRA interpretation is given in Table 1.

Table 1. Characteristics of various frequency response analysis (FRA) interpretation methods.

Proposed Methods	Advantages	Disadvantages
Statistical indicators [6–9]	- CC, ASLE, SD, SSE, MSE, and MM are used to distinguish two FRA traces. - CC and ASLE can give better comparison results	- CC is not sensitive to changes in the magnitude of the frequency response. - SD takes place when there is a normal slight shift in FRA peaks. - Others, MSE, MM, SSE, also have similar disadvantages to CC and SD. - Interpretation of the measured FRA still needs personnel expertise.
FRA modeling equivalent circuit [13–15]	- Can simulate the magnitude and phase of the FRA similar to the measured FRA. - This method can investigate major transformer faults such as radial deformation and axial displacement.	- Exact parameters should be identified by measurements or imperial equations. - The model cannot consider all transformer parameters, such as detailed mutual inductances and shunt conductance.

Table 1. *Cont.*

Proposed Methods		Advantages		Disadvantages
Mathematical models [16–18]	- -	They take into account the magnitude and phase of the FRA signature. The functions are not given in any particular order. It is a correct fit of the measurement.	- -	Transformers have different structures, so every transformer case needs a particular and complex mathematical model. Interpretation of the measured FRA still needs an expert.
ANNs [19–21]	-	ANNs help estimate the transformer winding RLC values using the FRA trace.	-	Applicability is limited due to its complexity.
Proposed guidelines in this study	- - -	Easy to use by inexperienced engineers Presents major transformer faults The proposed table shows the directions of response due to fault in three frequency regions.	-	Further validation for practical application is required.

This paper aims to take a step towards establishing guidelines for FRA interpretation. The proposed guidelines are designed to facilitate an uncomplicated way to identify fault types within power transformers. The proposed guidelines are developed by reviewing major studies and standards for FRA interpretation. The effect of various faults on a transformer FRA signature is categorized into three frequency bands: low, mid, and high. Classification is also categorized into three states: no variation, small variation, and large variation, through CC calculation. Non-expert users can use these guidelines to interpret the measured FRA responses. The proposed guidelines are validated through experimental testing on a three-phase 11/0.433 kV, 500 kVA distribution transformer with a short circuit fault. The step-by-step research progress of the proposed method is shown in Figure 1.
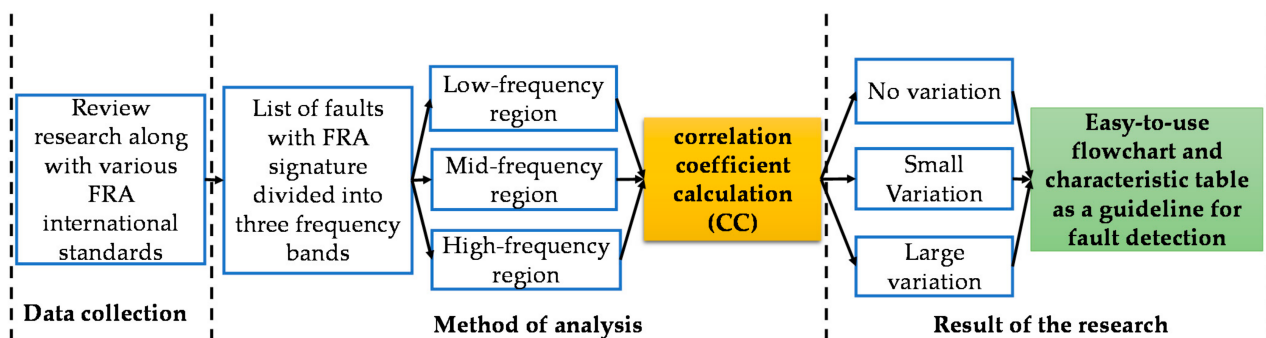

Figure 1. Steps and procedures of the proposed method.

2. Transformer Frequency Response Analysis

The principal function of the FRA is to detect winding and core deformation. Nowadays, the FRA test is recommended to be performed before and after transportation or relocation, on suspected units, and during regular offline maintenance.

The transformer frequency response is obtained by injecting a low (<20 V) AC input signal, 'V_{in}', of varying frequency at one terminal of a transformer winding [30]. The output voltage, 'V_{out}', is measured at the other terminal of the same winding, as shown in Figure 2. The frequency response, usually the transfer function, '$H(f)$', of V_{out} to V_{in}, is plotted as phase, '$\theta(f)$', and magnitude, '$K(f)$', in dB, in a frequency range of 2 MHz

as given by (1) and (2). The most commonly used plot for analyzing the response is the magnitude plot.

$$K(f) = 20 \log_{10} \frac{V_{out}}{V_{in}} \tag{1}$$

$$\phi(f) = \tan^{-1} \frac{\angle V_{out}}{\angle V_{in}} \tag{2}$$
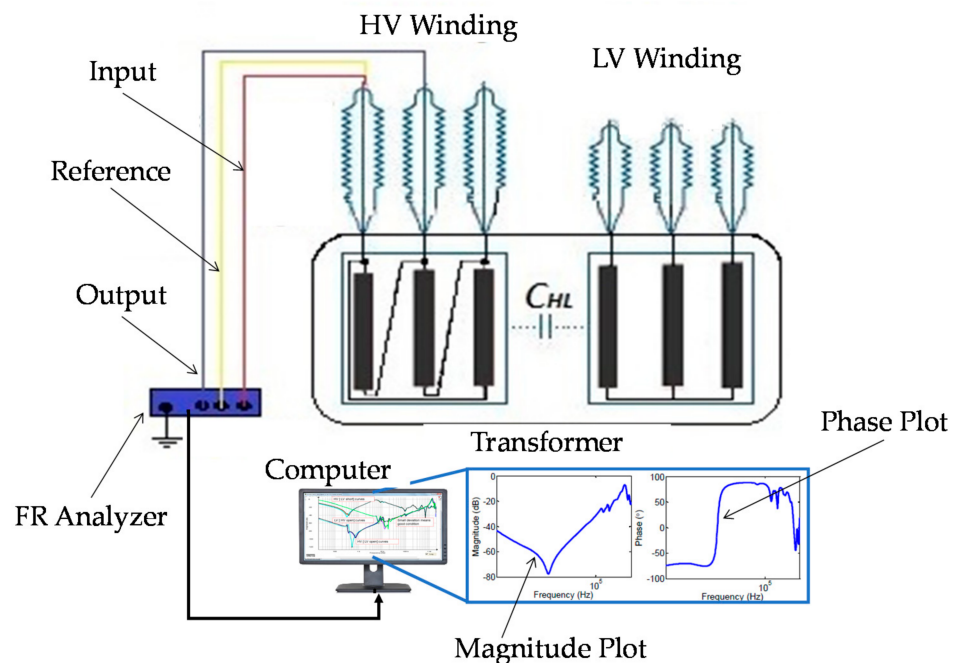

Figure 2. FRA test setup for transformer winding at end-to-end open circuit test [10].

FRA test configuration refers to the connection of the frequency response analyzer to the transformer. According to CIGRE WG A2/26 [2], IEEE Std. C57.149-2012 [1], and IEC 60076-18 [3], four different configurations can be used to perform FRA measurement. These are the end-to-end open circuit test, the end-to-end short circuit test, the capacitive inter-winding test, and the inductive inter-winding test.

The end-to-end open circuit configuration is performed by injecting the signal into one end of the winding and measuring the transmitted signal at the other end of the same winding. This configuration is commonly used because it can provide more information regarding the winding and core. An example of a typical frequency response using end-to-end open circuit configuration is shown in Figure 3a. On the other hand, in the end-to-end short circuit configuration, the secondary winding of the same phase is shorted to eliminate the influence of the core on the measurement, since the low-frequency response results from the magnetizing inductance of the iron core [25]. The typical frequency response of end-to-end short circuit configuration is shown in Figure 3b.

To interpret the FRA signature, it is necessary to analyze all frequency ranges. The frequency response can be divided into three regions as per IEC 60076-18 [3]: the low-frequency (LF) region, the mid-frequency (MF) region, and the high-frequency (HF) region, as shown in Figure 4. These responses are from measurements using end-to-end open and short circuit tests. However, there is no general frequency limit specified for each region as this mainly depends on the size and rating of the transformer. In the IEEE std. C57.104 [1], the frequency sub-bands are divided into four regions. The fourth region is for frequencies above 1 MHz, in which the effects of measurement and grounding leads are considerable.

It is crucial to analyze each frequency region because each frequency region is affected by different transformer faults. The core dominates the LF region, the MF region is

dominated by the parallel capacitance and mutual inductances, while the HF region is influenced by the winding capacitance [25,31].
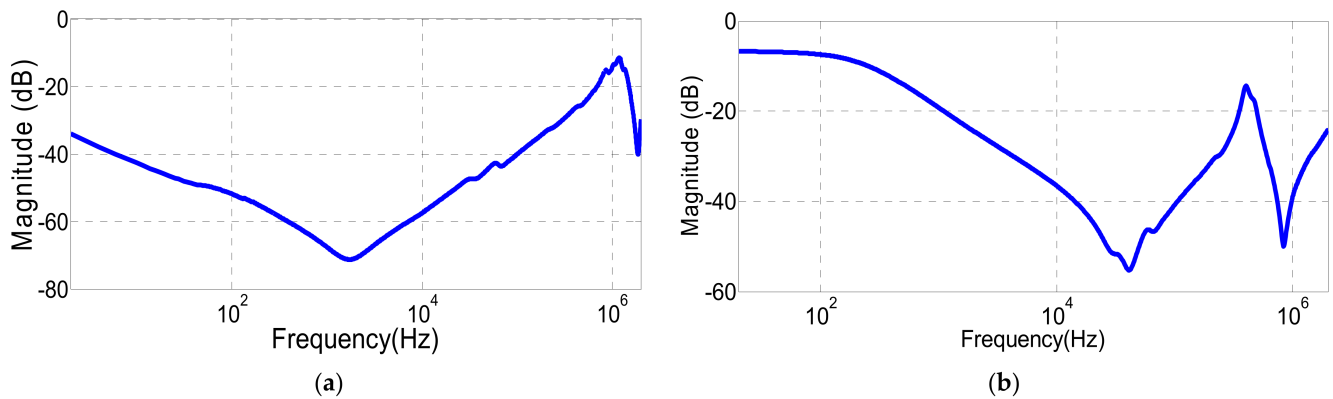

Figure 3. End—to—end measurement result from 500 kVA transformer: (**a**) open circuit test response, and (**b**) short circuit test response.
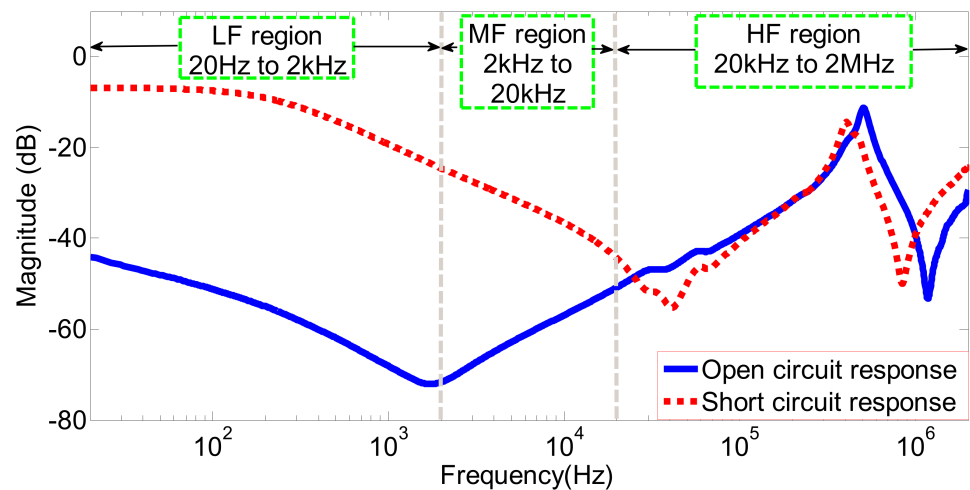

Figure 4. The three typical frequency sub—bands for transformer FRA.

Essentially, the frequency response of a transformer can be simulated based on a complex circuit consisting of resistances, inductances, capacitances, and mutual inductances, as shown in Figure 5. Each of the circuit elements is related to the physical geometry of the transformer winding [32,33].

In the transformer-equivalent high-frequency circuit shown in Figure 5, Rs, Cs, and Ls are the winding series resistance, capacitance, and self-inductance, respectively. Cg and Gg are the ground capacitance and conductance that represent the dielectric insulation system. M_{ij} is the mutual inductance. C_{HL} and G_{HL} are the capacitance and conductance between high voltage and low voltage windings.

Any changes in the winding will affect the RLC network, thereby altering the original or baseline frequency response [34]. The simulated frequency response of a simple RLC circuit is shown in Figure 6a. The winding resistance, 'R', contributes to the horizontal line, as shown in Figure 6b. The winding inductance, 'L', influences the negative slope illustrated in Figure 6c, at the low- and mid-frequency regions. The capacitive effect due to winding insulation affects the positive slope, shown in Figure 6d, at the mid- and high-frequency regions.
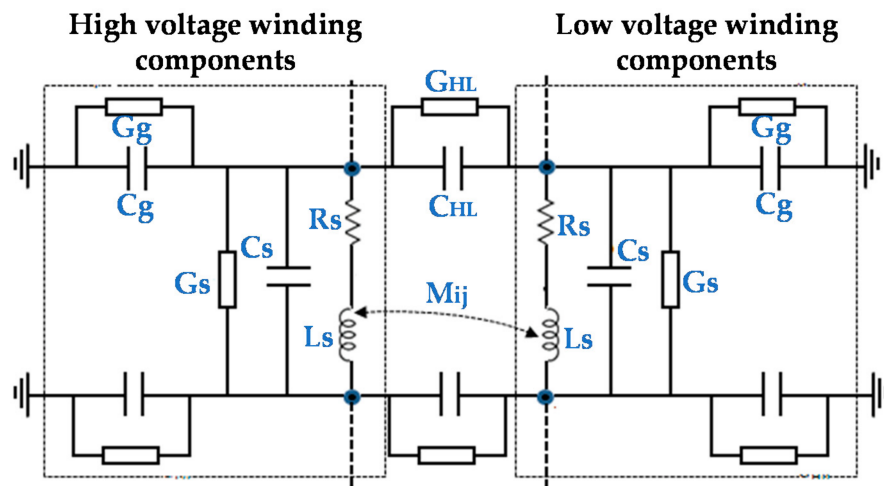
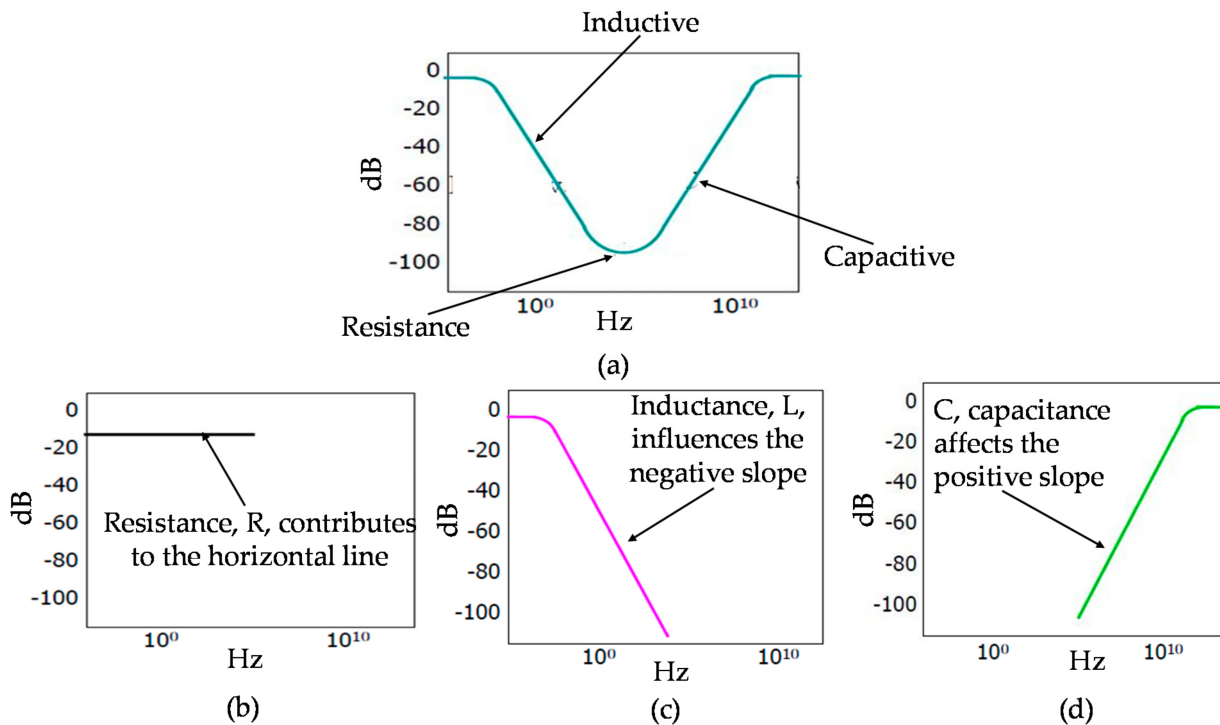**Figure 5.** The resistance, inductance, and capacitance (RLC) ladder network for single disc wind—ing [30].

Figure 6. (**a**) Resistance, inductance, and capacitance (RLC) circuit simulated response, (**b**) effect of resistance, (**c**) effect of inductance, and (**d**) effect of capacitance.

3. Fault Extent Methodology

This paper proposes three steps, or phases, for interpreting the FRA measurement, as shown in Figure 7. In phase 1, the response is divided into three frequency regions: the low-frequency region (LF < 2 kHz), the mid-frequency region (2 kHz < MF < 20 kHz) and the high-frequency region (HF > 20 kHz). Phase 2 determines the level of variation between the measured response and the reference signature by calculating the correlation coefficient (CC) that results in three categories. In [35–37], three CC limits are suggested to identify the transformer condition. The transformer is considered in good condition for a CC more than 0.98. The transformer health state is considered marginal for a CC in the range (0.96–0.97), and the transformer calls for further investigation for a CC less than or equal to 0.96. These limits are categorized based on the variation between the measured

and reference responses, which can be categorized into no variation, small variation, and large variation. The limits or range for the CC variation are given in Table 2.
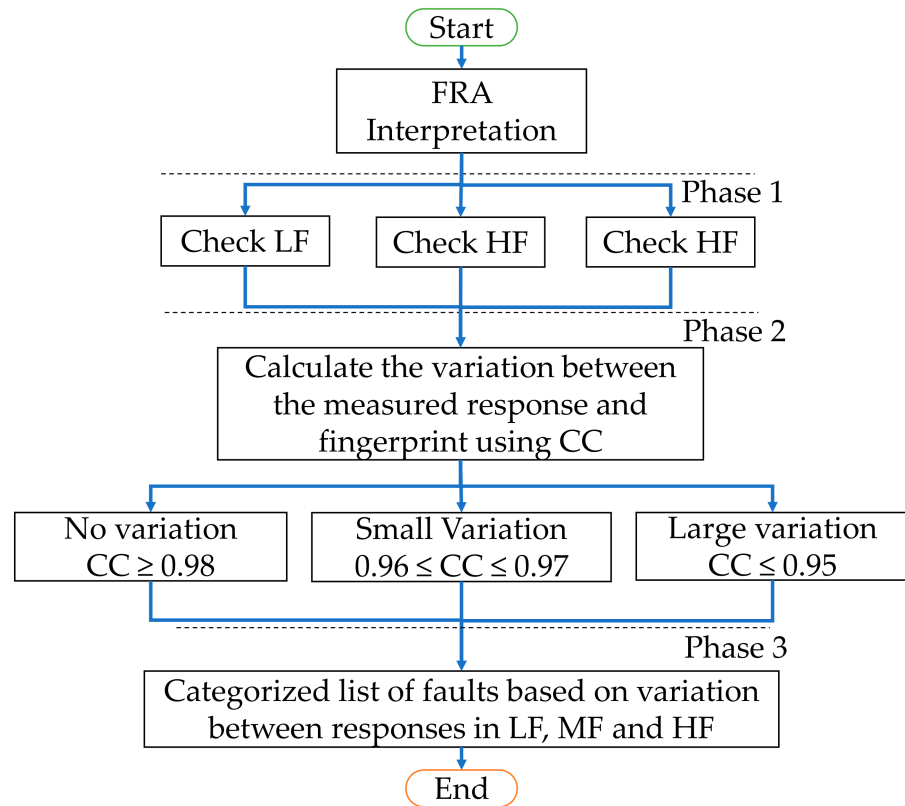

Figure 7. The proposed methodology for fault extent using the correlation coefficient (CC).

Table 2. CC benchmark limits and level of variation.

CC Value	Variation Level
0.98–1.00	No Variation
0.96–0.97	Small Variation
≤ 0.95	Large Variation

No variation means that the compared FRA responses are identical with a calculated CC of more than 0.98, as shown in Figure 8a. The small variation refers to cases when the CC ranges between 0.96 and 0.97. For large variation, the difference between the measured and baseline responses results in a CC less than 0.95, as shown in Figure 8b. In phase 3, the fault is estimated based on the CC levels for each frequency region.

Equation (3) is used to calculate CC. The value approaches 0 or 1 when the two responses are uncorrelated or identical, respectively. In Equation (3), *n* is the number of frequency points, and *x(i)* and *y(i)* are the two compared responses.

$$CC_{(x,y)} = \frac{\sum_{i=1}^{n} x(i) \times y(i)}{\sqrt{\sum_{i=1}^{n} [x(i)]^2 \times \sum_{i=1}^{N} [y(i)]^2}} \tag{3}$$
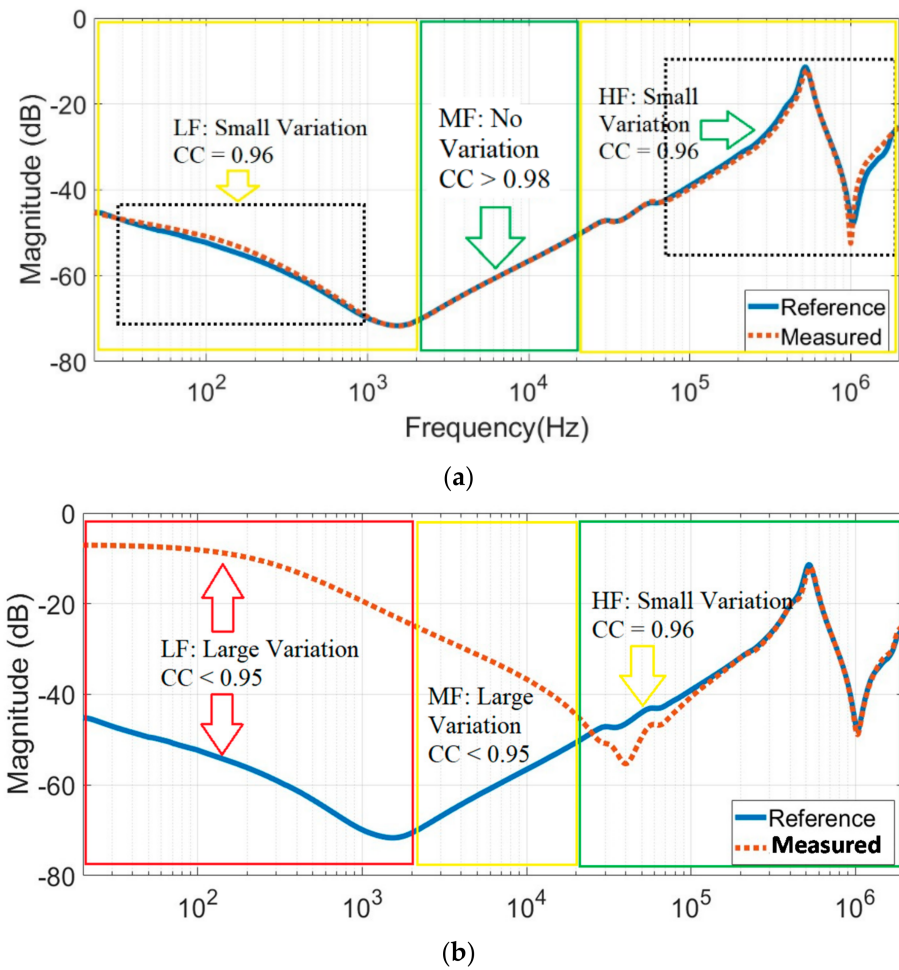
Figure 8. Example of variation between the measured and reference frequency responses: (**a**) small variation and (**b**) considerable or large variation.

4. Proposed Fault Identification Guidelines

The most common transformer faults and their impacts on various frequency bands based on extensive literature studies are listed in Table 3. Only end-to-end open and short circuit tests are considered in the study, as these are the most common essential test configurations as per the IEEE and IEC standards. Each of the faults listed in Table 3 has a distinct effect on the transformer frequency response. For example, core defects show a large variation at the low-frequency region, small variation at the mid-frequency region, and no variation at the high-frequency region.

Table 3. Effect of various transformer conditions on three frequency regions of the FRA signature.

NO	Sensitivity to Fault	Test Type	LF	MF	HF	Reference
1	Radial winding deformation	Short circuit test	No	Small	Large	[1,3]
2	Axial winding deformation	Short circuit test	No	Small	Small	[1,3,38,39]
3	Bulk winding deformation	Open circuit test	No	Large	No	[1,3,36]
4	Core defects	Open circuit test	Large	Small	No	[1–3,36]
5	Higher contact resistance	Open circuit test	No	Small	Small	[1,36]
6	Short circuit fault	Short circuit test	Small	Large	No	[1,2,36]
7	Inter-disc fault	Short circuit test	No	Small	Large	[22]
8	Open circuit winding	Open circuit test	No	Large	Small	[1,39]
9	Winding looseness due to transportation	Open circuit test	No	Small	Large	[1]
10	Floating shield with local insulation	Open circuit test	Small	Small	Large	[1,2]
11	Presence of oil	Open circuit test	No	Large	Large	[2,40,41]
12	Measurement direction	Open circuit test	No	No	Large	[3]

Table 3. *Cont.*

NO	Sensitivity to Fault	Test Type	LF	MF	HF	Reference
13	Effect of temperature	Open circuit test	Small	Small	Small	[3,41]
14	Loss of clamping pressure	Short circuit test	No	No	Small	[13]
15	Tap changer coking	Open circuit test	Large	No	No	[42]
16	Tap changer pitting	Open circuit test	Small	Small	Small	[42]
17	Winding insulation degradation	Open circuit test	No	No	Large	[43,44]
18	Clamping structure damage	Open circuit test	No	Small	No	[36]
19	High voltage bushing fault	Short circuit test	No	Small	Small	[5,39,40,44]
20	Increasing moisture content	Short circuit test	Small	Small	Small	[41,43,45]
21	Bad measurement practice	Open and short test	Large	Large	Large	[3]
22	No faults	Open and short test	No	No	No	Obvious

The proposed flowchart shown in Figure 9 is constructed based on Table 3. This flowchart can be adopted to determine the possible type of fault when comparing the FRA measurements at different frequency regions. The flowchart may indicate an "undefined" condition for certain frequency response variations that have not been recorded previously.
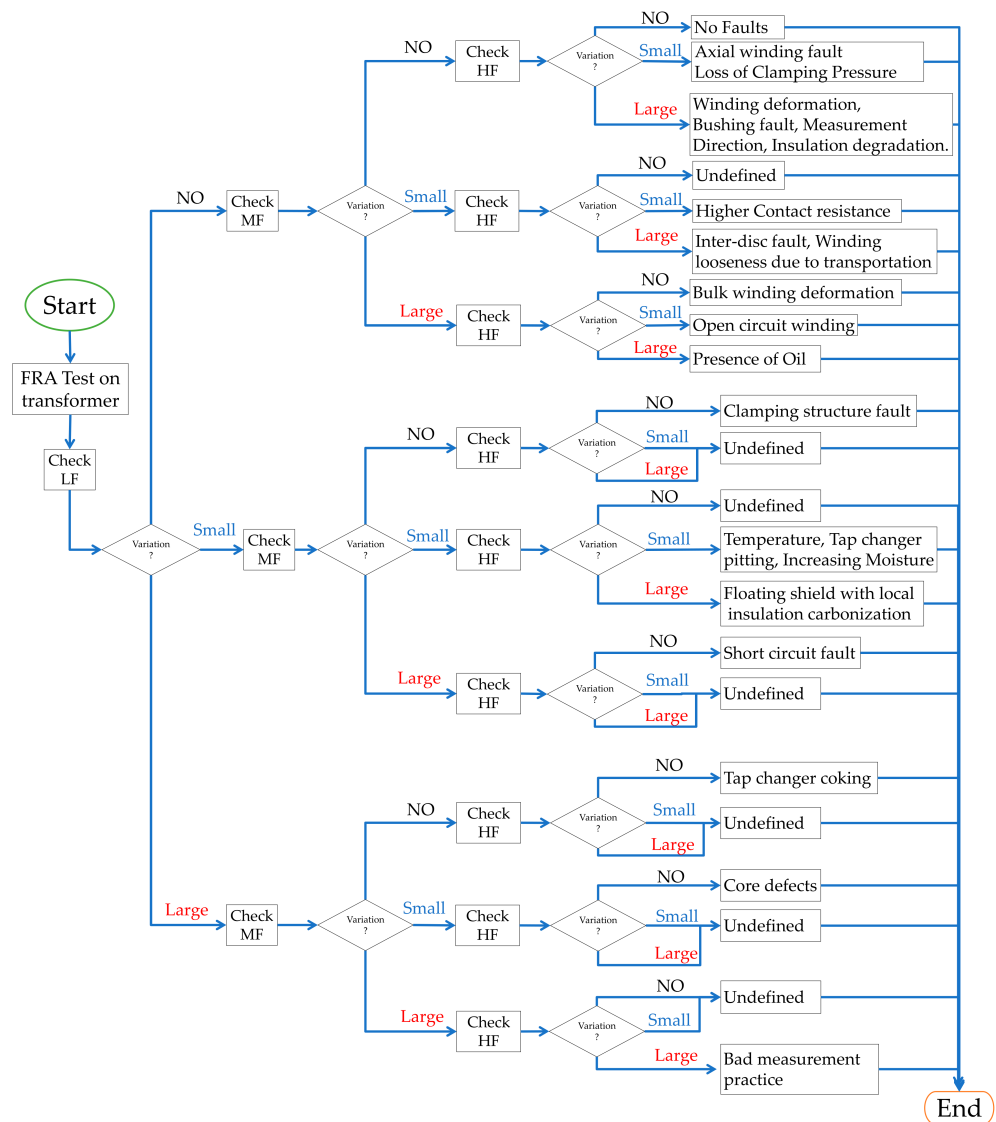

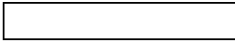**Figure 9.** The proposed FRA interpretation flowchart.

Table 4 provides additional information for FRA interpretation. It shows the change in the frequency response due to various faults. The proposed table describes how each

fault type impacts the frequency and magnitude by using a simple arrow, the direction of which indicates the deviation of the measured response compared to the reference FRA signature. Right direction arrows show that the measured response is shifted towards higher frequencies, while left direction arrows indicate a lower frequency movement. On the other hand, up and down arrows indicate an increase and decrease in response magnitude. The severity of variation is identified by the arrow shading degree, as shown in Table 4.

Table 4. Characteristics of FRA signature due to transformer faults.

Faults	Test Type	Magnitude			Shifting Frequency		
		LF	MF	HF	LF	MF	HF
Radial winding deformation	Short circuit test	-	-	↑	-	-	→
Axial winding deformation	Short circuit test	-	-	↑	-	-	←
Bulk winding deformation	Open circuit test	-	-	-	-	→	-
Core defects	Open circuit test	↓	↓	-	←	-	-
Higher contact resistance	Open circuit test	-	↑	↑	-	←	←
Short circuit fault	Short circuit test	↑	↑	-	→	→	-
Inter-disc fault	Short circuit test	-	↑	↑	-	→	→
Open circuit winding	Open circuit test	-	↓	↓	-	←	←
Winding looseness	Open circuit test	-	-	↑	-	→	→
Floating shield with local insulation	Open circuit test	-	-	↓	-	→	→
Presence of oil	Open circuit test	-	-	-	-	←	←
Measurement direction	Open circuit test	-	-	↓	-	-	-
Effect of high temperature	Open circuit test	-	-	-	←	←	←
Loss of clamping pressure	Short circuit test	-	-	↓	-	-	-
Tap changer coking	Open circuit test	↓	-	-	-	-	-
Tap changer pitting	Open circuit test	-	-	-	→	→	→
Winding insulation degradation	Open circuit test	-	-	-	-	-	←
Clamping structure damage	Open circuit test	↓	-	-	-	-	-
High voltage bushing fault	Short circuit test	-	-	↑	-	-	-
Increasing moisture content	Short circuit test	-	-	-	←	←	←
Bad measurement practice	Open and short test	↓↑	↓↑	↓↑	←→	←→	←→

-: No changes; ↓: Decrease; ↑: Increase; ←: Shifting towards lower frequencies; →: Shifting towards higher frequencies.

☐ No variation.　　☐ Small variation.　　☐ Large variation.

5. Case Study: Short Circuit Fault

For examining the feasibility of the proposed flowchart in Figure 9, laboratory testing was conducted on an 11/0.433 kV, 500 kVA transformer, as shown in Figure 10. The transformer windings were lifted from the main tank to access the tap changer. A short circuit fault in the winding was then created by shorting tap terminals 2–7 in-phase (R), as shown in Figure 11. A turns ratio test was performed on the transformer before and after applying the fault. The results of the measured V-ratio are presented in Table 5.

The FRA measurement was performed using a commercial frequency response analyzer on the tested winding open-circuit configuration before and after applying the short circuit fault, as shown in Figure 12. The fault causes shifting of the response at the low and mid-frequency regions toward higher frequencies, which is attributed to the reduction in the inductive components due to the shorted turns. Similarly, within the low and mid-frequency regions, the magnitude increases due to reduced inductance from the shorted turns. These changes align well with the variations listed in Table 4.

The CC between the FRA signatures for normal and short circuit faults was calculated to quantify the fault severity, and the result is shown in Table 6. Based on the proposed CC margins given in Figure 8 and Table 2, the results show a small variation at the low-frequency region, large variation in the mid-frequency region, and no variation in the high-frequency region. This is consistent with the short circuit fault identification using the proposed flowchart in Figure 9.
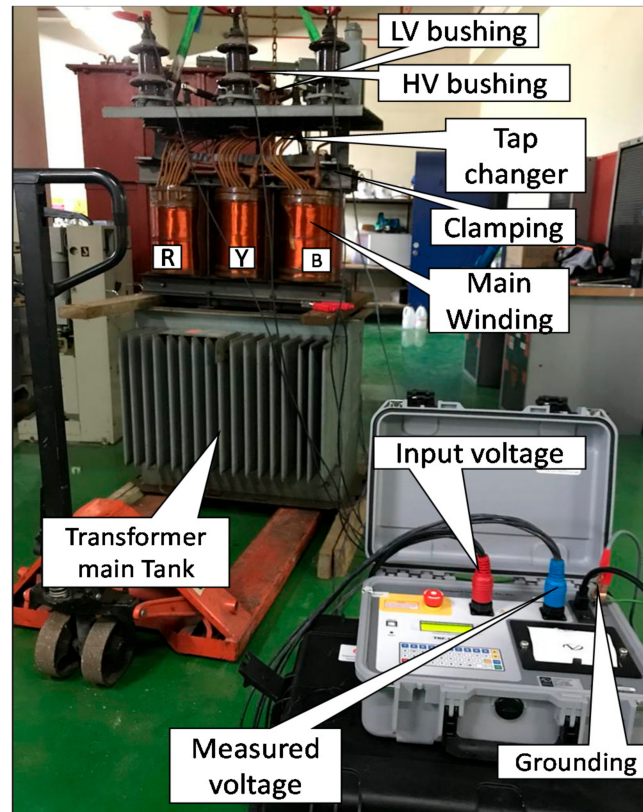

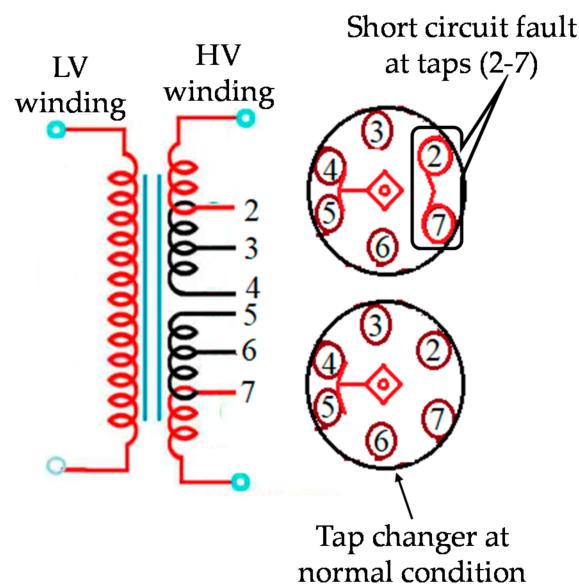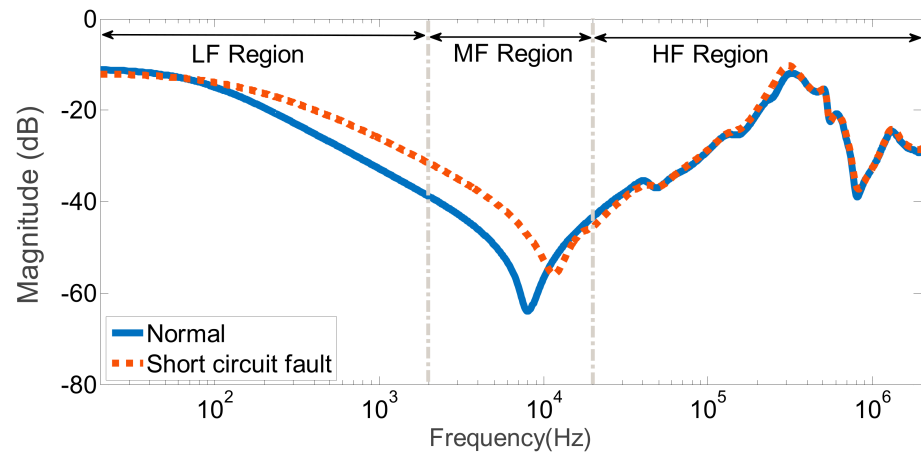**Figure 10.** The 500 kVA distribution transformer used in the case study.

Figure 11. Measurement setup at normal and short circuit fault conditions.

Table 5. Measured V-ratio at normal and faulty conditions.

Tap	HV Rating	Tap Connection	LV Rating	V-Ratio Normal	V-Ratio Fault
1	11,550	4–5	433	46.201	42.772

Figure 12. Measured FRA for normal and short circuit faults.

Table 6. Correlation coefficient results.

Frequency Range	CC Value
20 Hz–2 kHz	0.9842
2 kHz–20 kHz	0.6483
20 kHz–2 MHz	0.9965

6. Conclusions

FRA is a reliable tool for the assessment of power transformer mechanical integrity. However, FRA signature interpretation is still challenging due to the lack of easy and straightforward guidelines. This paper proposes an easy-to-use flowchart and characteristic table as a guideline to facilitate the identification and quantification of FRA signatures. The proposed guidelines are achieved according to the following points:

- The proposed guidelines are established based on the review of previous extensive research presented in the literature, along with various FRA international standards.
- The flowchart is developed based on three frequency regions and three levels of variations based on CC calculation.
- The characteristic table is presented graphically with arrows to provide a simple interpretation scheme for an inexperienced user.
- An experimental case study conducted on an 11/0.433 kV 500 kVA transformer with normal and short circuit faults is presented to verify the feasibility of the proposed guidelines.

Experimental results show that the variations within the three frequency regions of the measured response are consistent with the proposed guidelines. The proposed FRA guidelines can be used to identify approximately twenty-two transformer faults and conditions. Further feasibility studies should be conducted to investigate the accuracy of using the proposed method in practical case studies. Additionally, proposed guidelines should be analyzed and tested on different power transformers of various ratings and winding configurations.

Author Contributions: Conceptualization, S.M.A.-A. and M.F.M.Y.; methodology, S.M.A.-A., M.F.M.Y. and M.S.K.; software, S.M.A.-A. and M.F.M.Y.; validation, S.M.A.-A. and M.F.M.Y.; investigation, S.M.A.-A., M.F.M.Y. and M.S.K.; resources, S.M.A.-A. and M.F.M.Y.; writing—original draft preparation, S.M.A.-A. and M.F.M.Y.; writing—review and editing, M.F.M.Y., M.S.K., A.A.S. (Ali A. Salem),

References

1. IEEE. *C57.149-2012—Guide for the Application and Interpretation of Frequency Response Analysis for Oil-Immersed Transformers*; IEEE: Piscataway Township, NJ, USA, 2012. [CrossRef]
2. Picher, P. Mechanical Condition Assessment of Transformer Windings Using Frequency Response Analysis (Fra). *Cigre Eval.* **2008**, *26*, 30–34. Available online: https://www.scribd.com/doc/207245891/CiGRE-342-2008 (accessed on 2 October 2020).
3. IEC 60076-18 Ed. 1. Power Transformers—Part 18: Measurement of Frequency Response. 2012. Available online: https://webstore.iec.ch/publication/597 (accessed on 2 October 2020).
4. Frequency Response Analysis on Winding Deformation of Power Transformers. DL/T911-2016, (In Chinese), People Republic China, Electricity Power Industry Stand. 2016. Available online: https://www.codeofchina.com/standard/DLT911-2016.html (accessed on 2 October 2020).
5. Alsuhaibani, S.; Khan, Y.; Beroual, A.; Malik, N.H. A Review of Frequency Response Analysis Methods for Power Transformer Diagnostics. *Energies* **2016**, *9*, 879. [CrossRef]
6. Senobari, R.K.; Sadeh, J.; Borsi, H. Frequency response analysis (FRA) of transformers as a tool for fault detection and location: A review. *Electr. Power Syst. Res.* **2018**, *155*, 172–183. [CrossRef]
7. Secue, J.; Mombello, E. Sweep frequency response analysis (SFRA) for the assessment of winding displacements and deformation in power transformers. *Electr. Power Syst. Res.* **2008**, *78*, 1119–1128. [CrossRef]
8. Sant'Ana, W.C.; Salomon, C.P.; Lambert-Torres, G.; da Silva, L.E.B.; Bonaldi, E.L.; Oliveira, L.E.D.L.D.; da Silva, J.G.B. A survey on statistical indexes applied on frequency response analysis of electric machinery and a trend based approach for more reliable results. *Electr. Power Syst. Res.* **2016**, *137*, 26–33. [CrossRef]
9. Banaszak, S.; Kornatowski, E.; Szoka, W. The Influence of the Window Width on FRA Assessment with Numerical Indices. *Energies* **2021**, *14*, 362. [CrossRef]
10. Cheng, B.; Wang, Z.; Crossley, P. Using Lumped Element Equivalent Network Model to Derive Analytical Equations for Interpretation of Transformer Frequency Responses. *IEEE Access* **2020**, *8*, 179486–179496. [CrossRef]
11. Zhao, Z.; Yao, C.; Tang, C.; Li, C.; Yan, F.; Islam, S. Diagnosing Transformer Winding Deformation Faults Based on the Analysis of Binary Image Obtained From FRA Signature. *IEEE Access* **2019**, *7*, 40463–40474. [CrossRef]
12. Al-Ameri, S.; Yousof, M.F.M.; Azis, N.; Avinash, S.; Talib, M.A.; Salem, A.A. Modeling frequency response of transformer winding to investigate the influence of RLC. *Indones. J. Electr. Eng. Comput. Sci.* **2019**, *14*, 219–229. [CrossRef]
13. Abu-Siada, A.; Hashemnia, N.; Islam, S.; Masoum, M.A. Understanding power transformer frequency response analysis signatures. *IEEE Electr. Insul. Mag.* **2013**, *29*, 48–56. [CrossRef]
14. Murthy, A.S.; Azis, N.; Jasni, J.; Othman, M.L.; Yousof, M.F.M.; Talib, M.A. Extraction of winding parameters for 33/11 kV, 30 MVA transformer based on finite element method for frequency response modelling. *PLoS ONE* **2020**, *15*, e0236409. [CrossRef]
15. Abu-Siada, A.; Mosaad, M.I.; Kim, D.W.; El-Naggar, M.F. Estimating Power Transformer High Frequency Model Parameters Using Frequency Response Analysis. *IEEE Trans. Power Deliv.* **2019**, *35*, 1267–1277. [CrossRef]
16. Aljohani, O.; Abu-Siada, A. Application of Digital Image Processing to Detect Short-Circuit Turns in Power Transformers Using Frequency Response Analysis. *IEEE Trans. Ind. Informatics* **2016**, *12*, 2062–2073. [CrossRef]
17. Gonzales, J.C.; Mombello, E.E. Fault Interpretation Algorithm Using Frequency-Response Analysis of Power Transformers. *IEEE Trans. Power Deliv.* **2015**, *31*, 1034–1042. [CrossRef]
18. Trela, K.; Gawrylczyk, K.M. FEM Modelling of the Influence of the Remaining Windings on the Frequency Response of the Power Transformer. *Appl. Sci.* **2020**, *10*, 7633. [CrossRef]
19. Areu, O.H.; Menendez, A.M.G.; Sanchez, J.I.H.; Valdes, E.S. Diagnosis of faults in power transformers through the interpretation of FRA testing with artificial intelligence. In Proceedings of the 2018 IEEE International Autumn Meeting on Power, Electronics and Computing (ROPEC), Ixtapa, Mexico, 14–16 November 2018. [CrossRef]

20. Gutten, M.; Korenciak, D.; Kucera, M.; Janura, R.; Glowacz, A.; Kantoch, E. Frequency and time fault diagnosis methods of power transformers. *Meas. Sci. Rev.* **2018**, *18*, 162–167. [CrossRef]

21. Abu-Siada, A.; Radwan, I.; Abdou, A.F. 3D approach for fault identification within power transformers using frequency response analysis. *IET Sci. Meas. Technol.* **2019**, *13*, 903–911. [CrossRef]

22. Tahir, M.; Tenbohlen, S. A Comprehensive Analysis of Windings Electrical and Mechanical Faults Using a High-Frequency Model. *Energies* **2019**, *13*, 105. [CrossRef]

23. Banaszak, S.; Szoka, W. Cross Test Comparison in Transformer Windings Frequency Response Analysis. *Energies* **2018**, *11*, 1349. [CrossRef]

24. Yousof, M.F.M.; Al-Ameri, S.; Ahmad, H.; Illias, H.A.; Arshad, S.N.M. A New Approach for Estimating Insulation Condition of Field Transformers Using FRA. *Adv. Electr. Comput. Eng.* **2020**, *20*, 35–42. [CrossRef]

25. Omicron, F.P. *Interpretation of Sweep Frequency Response Analysis (SFRA) Measurement Results*; OMICRON Energy: Bundoora, Australia, 2016; pp. 1–26. Available online: https://www.ee.co.za/article/interpreting-sweep-frequency-response-analysis-measurements.html (accessed on 15 October 2020).

26. Bustamante, S.; Manana, M.; Arroyo, A.; Laso, A.; Martinez, R. Determination of Transformer Oil Contamination from the OLTC Gases in the Power Transformers of a Distribution System Operator. *Appl. Sci.* **2020**, *10*, 8897. [CrossRef]

27. Murthy, A.S.; Azis, N.; Al-Ameri, S.; Yousof, M.F.M.; Jasni, J.; Talib, M.A. Investigation of the Effect of Winding Clamping Structure on Frequency Response Signature of 11 kV Distribution Transformer. *Energies* **2018**, *11*, 2307. [CrossRef]

28. Al-Ameri, S.; Alawady, A.A.; Yousof, M.F.M.; Ahmad, H.; Salem, A.A.; Talib, M.A. Frequency response analysis for transformer tap changer damage detection. *Int. J. Power Electron. Drive Syst. (IJPEDS)* **2020**, *11*, 350–358. [CrossRef]

29. Liu, J.; Zhao, Z.; Tang, C.; Yao, C.; Li, C.; Islam, S. Classifying Transformer Winding Deformation Fault Types and Degrees Using FRA Based on Support Vector Machine. *IEEE Access* **2019**, *7*, 112494–112504. [CrossRef]

30. Zhao, Z.; Tang, C.; Yao, C.; Zhou, Q.; Xu, L.; Gui, Y.; Islam, S. Improved Method to Obtain the Online Impulse Frequency Response Signature of a Power Transformer by Multi Scale Complex CWT. *IEEE Access* **2018**, *6*, 48934–48945. [CrossRef]

31. Omicron. Performing reliable and reproducible frequency response measurements on power transformers. *Transform. Mag.* **2018**, *5*, 1–12.

32. Ćalasan, M.; Mujičić, D.; Rubežić, V.; Radulović, M. Estimation of Equivalent Circuit Parameters of Single-Phase Transformer by Using Chaotic Optimization Approach. *Energies* **2019**, *12*, 1697. [CrossRef]

33. Banaszak, S.; Gawrylczyk, K.M.; Trela, K. Frequency Response Modelling of Transformer Windings Connected in Parallel. *Energies* **2020**, *13*, 1395. [CrossRef]

34. Bagheri, M.; Nezhivenko, S.; Phung, B.T.; Blackburn, T. Air Core Transformer Winding Disk Deformation: A Precise Study on Mutual Inductance Variation and Its Influence on Frequency Response Spectrum. *IEEE Access* **2017**, *6*, 7476–7488. [CrossRef]

35. Bigdeli, M.; Siano, P.; Alhelou, H.H. Intelligent Classifiers in Distinguishing Transformer Faults Using Frequency Response Analysis. *IEEE Access* **2021**, *9*, 13981–13991. [CrossRef]

36. Kennedy, G.; McGrail, A.; Lapworth, J. Transformer sweep frequency response analysis (SFRA). *Energize* **2007**, 28–33. Available online: https://www.ee.co.za/wp-content/uploads/legacy/Transformer_.pdf (accessed on 25 October 2020).

37. Yousof, M.F.M.; Ekanayake, C.; Saha, T.K. Frequency response analysis to investigate deformation of transformer winding. *IEEE Trans. Dielectr. Electr. Insul.* **2015**, *22*, 2359–2367. [CrossRef]

38. Rahimpour, E.; Christian, J.; Feser, K.; Mohseni, H. Transfer function method to diagnose axial displacement and radial deformation of transformer windings. *IEEE Trans. Power Deliv.* **2003**, *18*, 493–505. [CrossRef]

39. Liu, S.; Liu, Y.; Li, H.; Lin, F. Diagnosis of transformer winding faults based on FEM simulation and on-site experiments. *IEEE Trans. Dielectr. Electr. Insul.* **2016**, *23*, 3752–3760. [CrossRef]

40. Hashemnia, N.; Abu-Siada, A.; Masoum, M.A.S.; Islam, S.M. Characterization of transformer FRA signature under various winding faults. In Proceedings of the 2012 IEEE International Conference on Condition Monitoring and Diagnosis, Bali, Indonesia, 23–27 September 2012; pp. 446–449. [CrossRef]

41. Reykherdt, A.A.; Davydov, V. Case studies of factors influencing frequency response analysis measurements and power transformer diagnostics. *IEEE Electr. Insul. Mag.* **2011**, *27*, 22–30. [CrossRef]

42. Al-Ameri, S.; Yousof, M.F.M.; Ahmad, H.; Alsubari, M.; Talib, M.A. Examining faulty transformer tap changer using frequency response analysis. In Proceedings of the International Symposium on Electrical Insulating Materials, Toyohashi City, Japan, 11–15 September 2017. [CrossRef]

43. Yousof, M.F.M.; Ekanayake, C.; Saha, T.K. Examining the ageing of transformer insulation using FRA and FDS techniques. *IEEE Trans. Dielectr. Electr. Insul.* **2015**, *22*, 1258–1265. [CrossRef]

44. Aljohani, O.; Abu-Siada, A. Identification of the minimum detection of transformer bushing failure based on Frequency Response Analysis (FRA). In Proceedings of the 2016 IEEE 2nd Annual Southern Power Electronics Conference (SPEC), Auckland, New Zealand, 5–8 December 2016; pp. 1–5. [CrossRef]

45. Bagheri, M.; Phung, B.; Blackburn, T. Influence of moisture content variation on Frequency Response Analysis of transformer winding. In Proceedings of the 2014 IEEE Electrical Insulation Conference (EIC), Philadelphia, PA, USA, 8–11 June 2014; pp. 333–337. [CrossRef]